Electronic Supplementary Material (ESI) for CrystEngComm

Supporting Materials

On polymorphism of 2-(4-fluorophenylamino)-5-(2,4-dihydroxybenzeno)-1,3,4-thiadiazole (FABT) DMSO Solvates

Anna A. Hoser[1§], Daniel M. Kamiński[2§], Arkadiusz Matwijczuk[3], Andrzej Niewiadomy[2], Mariusz Gagoś[3,4*], Krzysztof Woźniak[1*]

[1]Department of Chemistry, University of Warsaw, 02-093 Warszawa, Pasteura 1, Poland.
[2]Department of Chemistry, University of Life Sciences in Lublin, Akademicka 15, 20-950 Lublin, Poland.
[3]Department of Biophysics, University of Life Sciences in Lublin, Akademicka 13, 20-950 Lublin, Poland.
[4]Department of Cell Biology, Institute of Biology and Biochemistry, Maria Curie-Skłodowska University, 20-033 Lublin, Poland.

*Corresponding authors: Mariusz Gagoś (mariusz.gagos@up.lublin.pl)
Krzysztof Woźniak (kwozniak@chem.uw.edu.pl)

[§]Both authors contributed equally to this work

Hirshfeld surfaces. We used fingerprint plots generated from Hirshfeld surfaces [47] to compare interactions between neighbouring molecules in investigated solvates. The following weighing function is used to define a Hirshfeld surface:

$$w_A(\boldsymbol{r}) = \frac{\sum_{i \in \text{molecule } A} \rho_i(\boldsymbol{r} - \boldsymbol{r}_i)}{\sum_{i \in \text{crystal}} \rho_k(\boldsymbol{r} - \boldsymbol{r}_k)},$$

where ρ_i is the spherically averaged atomic electron density of the *i*-th atom in the molecule (centred at point $\boldsymbol{r}_i$) and ρ_k the electron density of *k*-th atom surrounding a particular molecule in the crystal. This weighing function defines the so-called Hirshfeld surface for molecule *A* when $w_A(\boldsymbol{r}) = 0.5$ for every point $\boldsymbol{r}$ at the surface. Within the Hirshfeld surface, the promolecule electron density dominates over the procrystal electron density. It is possible to map different properties on Hirshfeld surfaces: properties related to the shape of the surface (e.g. curvedness) and also those connected with distances: d_e – external distance from the Hirshfeld surface to an atom belonging to the closest molecules outside the surface, d_i- internal distance from the surface to an atom inside the surface and $d_{norm,}$ which combines both d_e and d_i, each normalised by the van der Waals (vdW) radius for the particular atoms involved in the close proximity to the surface. When d_e and d_i are calculated for each point of the Hirshfeld surface, a 2D (d_e vs d_i) a fingerprint plot can be created. The presented figures of Hirshfeld surface and fingerprint plots were prepared in CrystalExplorer program [48].

(a)

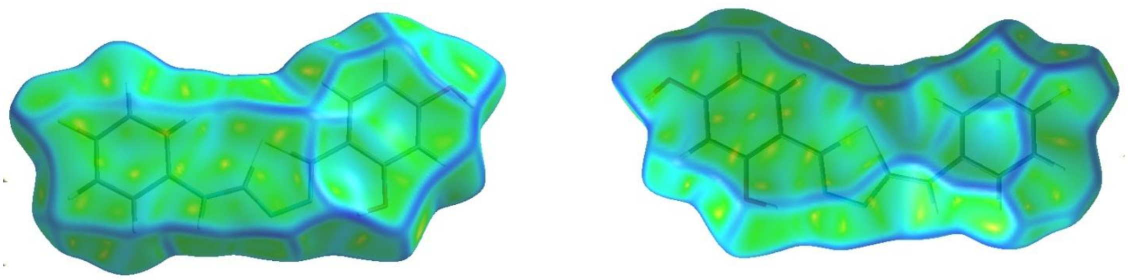

(b)

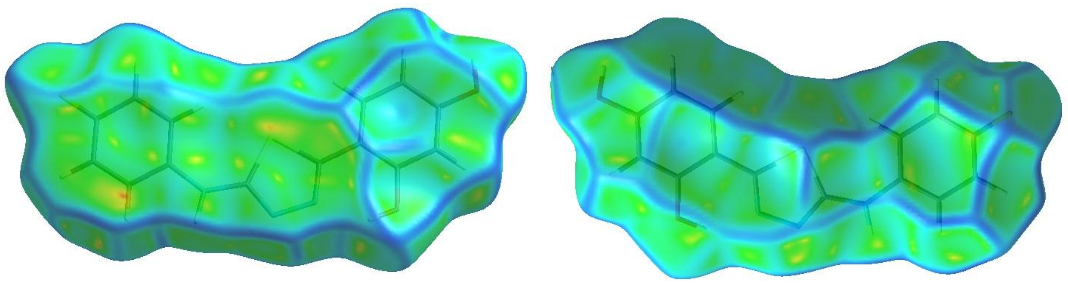

Figure 1S. Curvendness mapped on Hirshfeld surfaces for both sides of the (a) **FBxDM I** and (b) **FBxDM II** molecules**.**

Table 1S. Relative contributions of chosen intermolecular interactions to the Hirshfeld surface area for the **FABT** polymorphs.

	Percentage contribution of particular interactions at the Hirshfeld surface		
	FABT I	**FABT II**	**Difference**
F···H	8,7	9,7	-1
O···H	15,4	14,5	0,9
N···H	10,7	11,4	-0,7
S···H	5,5	4	1,5
C···H	12,7	21,6	-8,9
C···C	7	2,6	4,4
H···H	30	25,5	4,5
Other	10	10,7	-0,7

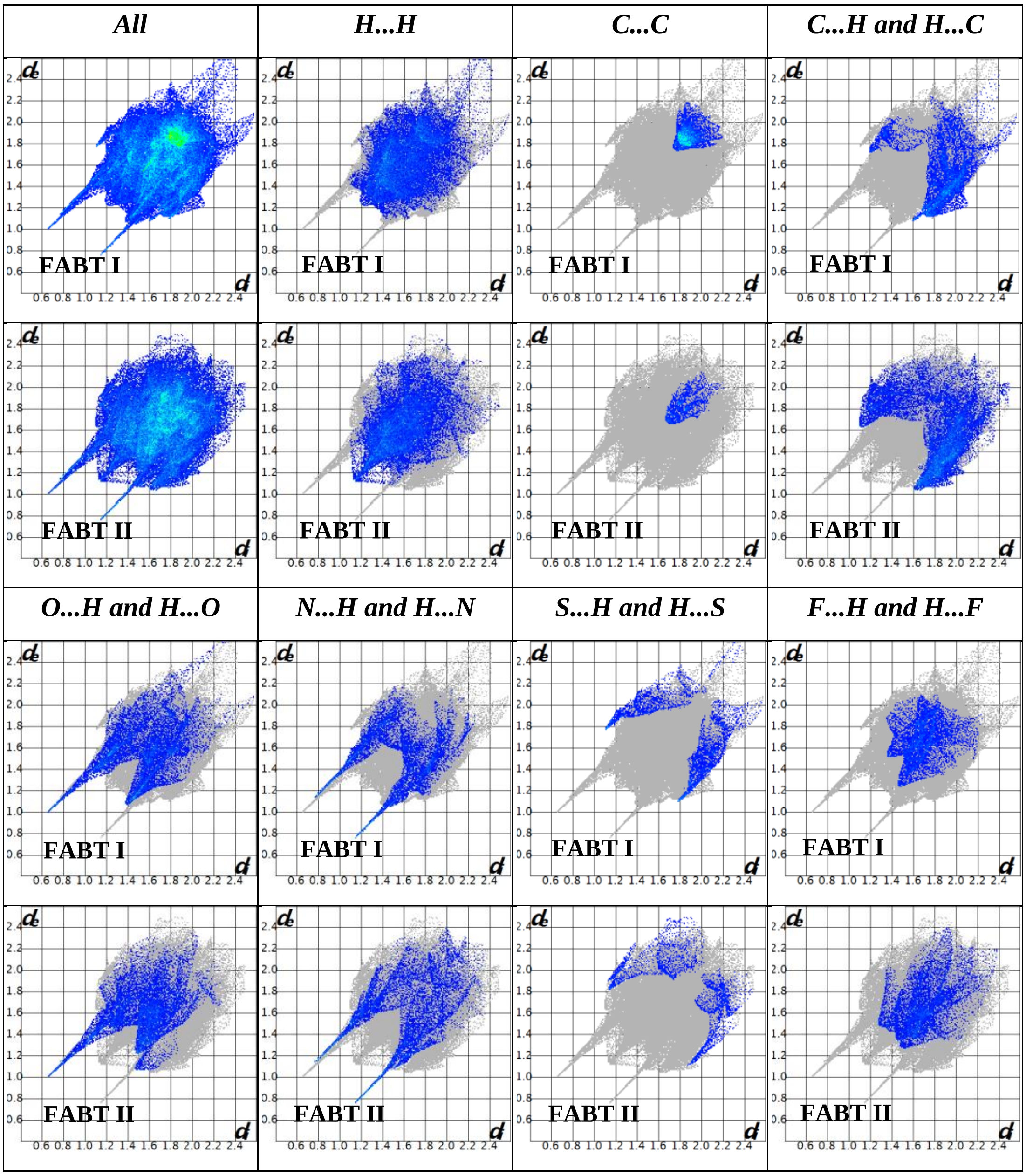

Figure 2S. Fingerprint plots and their breakdown into particular contributions.

Table 2S. Bond distances for **FABT** in the investigated polymorph structures of **FBxDM I** and **FBxDM II.**

Bond	FBxDM I	FBxDM II
S1-C7	1.740(2)	1.732(5)
S1-C8	1.750(2)	1.737(5)
S2-O1S	1.511(2)	1.508(3)
S2-C2S	1.769(3)	1.760(5)
S2-C1S	1.771(3)	1.783(5)
F1-C1	1.368(3)	1.363(5)
N3-C8	1.307(3)	1.296(6)
N3-N2	1.378(2)	1.376(5)
O2-C10	1.365(3)	1.363(6)
O1-C12	1.362(3)	1.355(5)
N2-C7	1.314(3)	1.315(6)
N1-C7	1.355(3)	1.352(6)
N1-C4	1.401(3)	1.409(6)
C14-C13	1.381(3)	1.389(6)
C14-C9	1.404(3)	1.379(7)
C8-C9	1.457(3)	1.457(6)
C2-C3	1.372(3)	1.369(7)
C2-C1	1.373(3)	1.362(7)
C9-C10	1.405(3)	1.399(7)
C5-C6	1.386(3)	1.388(7)
C5-C4	1.390(3)	1.371(7)
C10-C11	1.390(3)	1.383(6)
C12-C11	1.381(3)	1.371(7)
C12-C13	1.393(3)	1.399(7)
C4-C3	1.403(3)	1.396(6)
C6-C1	1.367(3)	1.372(7)

Table 3S. Valence angles in FABT molecules present in both polymorphs of FABT. Significant differences in red.

			FBxDM I	FBxDM II
C7	S1	C8	87.12(11)	87.1(2)
O1S	S2	C2S	104.76(12)	104.9(2)
O1S	S2	C1S	104.81(12)	105.3(2)
C2S	S2	C1S	99.17(16)	98.0(2)
C8	N3	N2	114.23(19)	115.0(4)
C7	N2	N3	111.94(18)	110.7(4)
C7	N1	C4	132.6(2)	131.6(4)
C13	C14	C9	121.3(2)	121.7(5)
N3	C8	C9	122.8(2)	123.2(4)
N3	C8	S1	112.66(17)	112.7(3)
C9	C8	S1	124.50(17)	124.2(4)
C3	C2	C1	118.8(2)	119.1(5)
C14	C9	C10	118.3(2)	118.5(4)
C14	C9	C8	121.8(2)	121.6(4)
C10	C9	C8	119.9(2)	120.0(4)
N2	C7	N1	118.7(2)	118.7(4)
N2	C7	S1	114.03(17)	114.5(3)
N1	C7	S1	127.28(18)	126.8(4)
C6	C5	C4	120.3(2)	120.3(4)
O2	C10	C11	116.9(2)	116.8(4)
O2	C10	C9	122.8(2)	122.4(4)
C11	C10	C9	120.3(2)	120.7(5)
O1	C12	C11	121.9(2)	118.0(4)
O1	C12	C13	117.6(2)	121.1(5)
C11	C12	C13	120.5(2)	120.9(4)
C12	C11	C10	120.2(2)	119.8(5)
C5	C4	N1	125.4(2)	124.5(4)
C5	C4	C3	119.0(2)	119.9(5)
N1	C4	C3	115.6(2)	115.6(4)
C2	C3	C4	120.6(2)	119.9(5)
C1	C6	C5	119.0(2)	118.1(5)
C14	C13	C12	119.4(2)	118.4(5)
C6	C1	F1	118.7(2)	118.0(5)
C6	C1	C2	122.4(2)	122.6(5)
F1	C1	C2	118.9(2)	119.4(4)

Table 4S. Details of hydrogen bonding and other strongest intermolecular interactions in **FBxDM I** and **FBxDM II** crystal lattices.

D-H···A	Symm	d(D-H) / Å	d(H···A) / Å	d(D···A) / Å	<DHA / °
FBxDM I					
N1-H1N...N2	**-x, -y, -z+2**	0.79(2)	2.13(2)	2.921(3)	171(2)
O2-H2O...N3	**x,y,z**	0.75(3)	1.93(3)	2.622(3)	153(3)
O1-H1O...O1S	**x-1, y-1,z-1**	0.90(3)	1.75(3)	2.644(3)	174(3)
Weak hydrogen bonds:					
C3-H3... N3	**-x, -y, -z+2**	0.95	2.65	3.520(3)	153
C6-H6...O1	**1-x, -y, 1-z**	0.95	2.55	3.254(3)	131
C14-H14...O2	**1+x, y, z**	0.95	2.63	3.411(3)	140
C1S-H11S...O2	**-x, -y, -z+2**	0.98	2.66	3.546(3)	150
FBxDM II					
N1-H1N...N2	**2-x, 2-y, -z**	0.86(5)	2.06(5)	2.918(6)	171(4)
O2-H2O...N3	**x, y, z**	0.86(5)	1.92(6)	2.601(5)	135(5)
O1-H1O...O1S	**x, y, z**	0.92(7)	1.74(7)	2.647(5)	168(6)
Weak hydrogen bonds:					
C1S-H13S...O2	**2-x, 1-y, 1-z**	0.98	2.67	3.627(6)	166
C1S-H13S...C10	**2-x, 1-y, 1-z**	0.98	2.84	3.738(6)	152
C3-H3...N3	**2-x, 2-y, -z**	0.95	2.72	3.599(6)	154